Macromolecules
ARTICLE

Macromolecules **2010**, *43*, 9635–9644 **9635**
DOI: 10.1021/ma101953h

A Simple Polymerizable Polysoap Greatly Enhances the Grafting Efficiency of the "Grafting-to" Functionalization of Multiwalled Carbon Nanotubes

Mao Peng,* Zhangjie Liao, Zhongming Zhu, and Honglei Guo

MOE Key Laboratory of Macromolecular Synthesis and Functionalization, Department of Polymer Science and Engineering, Zhejiang University, Hangzhou 310027, China

Received August 24, 2010; Revised Manuscript Received November 3, 2010

ABSTRACT: A simple polymerizable polysoap was synthesized for the functionalization of multiwalled carbon nanotubes (MWNTs) by "grafting to" method, which greatly enhances the grafting efficiency (i.e., the ratio between the quantity of grafted polymer and the total polymerized monomer). Self-assembly of MWNTs with the polysoaps in a 1,4-dioxane/water mixture results in the formation of micellized MWNTs; then, by a single step of polymerization of the polysoaps or copolymerization of the polysoaps with methyl methacrylate (MMA), the polymer layer of the micellized MWNTs is permanently cross-linked and covalently bonded to the nanotube surface. For the poly(polysoap-*co*-MMA) modified MWNTs, the grafting efficiency can be as high as 65.7%. The functionalized MWNTs are robust, readily redispersible in water and some organic solvents, and increase the dynamic mechanical properties of epoxy resin more effectively than oxidized or noncovalently modified MWNTs.

Introduction

In recent years, carbon nanotubes (CNTs), including both single-walled carbon nanotubes (SWNTs) and multiwalled carbon nanotubes (MWNTs), have been continuously attracting wide interests from both scientific and technological areas, due to their unique mechanical, electrical and thermal properties.[1] Surface modification or functionalization of CNTs has been actively pursued, which is crucial for preventing the aggregation of CNTs in solutions or polymer matrices and fully utilizing their unique properties. Both covalent and noncovalent functionalizations of CNTs have been developed for this purpose.[1,2]

In comparison with covalent functionalization, noncovalent functionalization of CNTs is relatively facile; for example, CNTs can be decorated by surfactants,[3,4] lipids,[5] pyrene derivatives,[6] block copolymers,[7] water-soluble polymers and derivatives,[8] and polysoaps[9,10] in selective solvents under very mild conditions. Polysoaps, as amphiphilic polymers with a hydrophilic backbone and hydrophobic side chains attached at regular intervals along the backbone,[11] are effective for wrapping CNTs in water. For example, Chen et al.[9] reported a polysoap synthesized by functionalizing the side chain of poly(styrene-*alt*-maleic acid) with aminopyrene, which can disperse SWNTs in water more effectively than DNA. However, different from covalent functionalizations, noncovalent functionalizations are often associated with relatively weak interactions between the nanotubes and the amphiphilic coatings. Under certain conditions, the coatings can be detached from the nanotube surfaces, leading to a reagglomeration. This is especially undesirable for the usage of CNTs as reinforcing agents for polymers.

By covalent functionalization, robust functionalized CNTs can be readily obtained. For instance, grafting macromolecular chains onto the surface of CNTs through either "grafting to"[12−17] or "grafting from"[18−20] routes have been proven to be effective for the functionalization of CNTs. For the "grafting to" methods, it has been demonstrated that both small molecular[11] and macromolecular free radicals[13] can be covalently attached to the sidewall of CNTs, while the grafting efficiency, i.e., the ratio between the quantity of grafted monomer and the total polymerized monomer, is usually relatively low. For example, the grafting efficiency by direct free radical addition in the good solvents of the grafted polymers is below 1% for MWNTs[14] and ranges from 0.6% to 13.4% for SWNTs.[15] The lower grafting efficiency for MWNTs is because of the much smaller specific surface area and lower reactivity of MWNTs in free radical addition reaction. As is generally accepted, the reactivity of CNTs largely depends on the curvature the sidewalls, and CNTs with larger diameters are less reactive.[16] The low grafting efficiency means that an extremely high monomer/CNTs ratio (typically 20:1−200:1)[14,15] is necessary to produce polymer-grafted CNTs with a satisfactory grafting amount of the polymers. An exception is the method reported by Wang et al.,[17] in which poly(methyl methacrylate) (PMMA) is grafted onto SWNTs in poor solvents of PMMA. Different from the polymerization in good solvents or solvent-free polymerization, the method increases the grafting efficiency up to 40% for SWNTs.

Compared with most "grafting to" methods, "grafting from" methods exhibit significantly higher grafting efficiencies (especially for living polymerization), because the polymer chains can be grafted more densely onto the convex walls of CNTs.[18−20] As reported by Baskaran and coauthors,[18] the grafting efficiency for living anionic surface-initiated polymerization of styrene and isoprene on MWNTs can be even as high as 100%. By *in situ* atom transfer radical polymerization (ATRP) or reversible addition and fragmentation chain transfer (RAFT) polymerization on MWNTs, the grafting efficiencies are 20−40%,[19] also much higher than by "grafting to" methods. Nevertheless, the "grafting from" methods usually involve two or more chemical steps, because initiators or catalysts must be immobilized onto the nanotube surfaces first before the graft polymerization.

In this study, we report a new "grafting to" method for the functionalization of MWNTs exhibiting high grafting efficiency under mild reaction conditions, basing on the combination of free

*To whom correspondence should be addressed. Fax: ++86-571-87953712. Telephone: ++86-571-87953712. E-mail: pengmao@zju.edu.cn.

Published on Web 11/18/2010

radical polymerization with the noncovalent functionalization of MWNTs by a new polymerizable polysoap, namely, a polysoap containing polymerizable vinyl groups. MWNTs are first micellized by the polymerizable polysoap in a selective solvent, then, by a single-step *in situ* polymerization of the polysoap or the copolymerization of the polysoap with a monomer methyl methacrylate (MMA) on the surface of MWNTs, robust and soluble polymer-encapsulated MWNTs are obtained. In comparison with common surfactants used for the noncovalent decoration of CNTs, the polymerizable polysoap is not only very effective for the micellization of MWNTs but can also be polymerized or copolymerized, thus, can be covalently bonded to the sidewall of CNTs. The grafting efficiency, i.e., the ratio between the quantity of grafted polymer and the total added polysoap and monomer, obtained by this method is much higher than that by conventional "grafting to" methods. Also, compared with noncovalently functionalized MWNTs, our modified MWNTs exhibit a greatly improved structural stability, redispersibility in water and organic solvents, and can more effectively improve the dynamic mechanical properties of epoxy resin. Different from some other chemical modifications of MWNTs, this method is facile, mild, and does not use harsh chemicals throughout the preparative procedure.

Experimental Section

Materials. MWNTs (purity >95 wt %, length ranges from 5 to 15 μm, BET surface area =216 m^2/g) was supplied by Shenzhen Nano-Technologies Port Co. Ltd. Styrene, MMA, maleic anhydride (MAn), benzoyl peroxide (BPO), 2,2′-azobis(isobutyronitrile) (AIBN), toluene, and 1,4-dioxane were purchased from China Medicine Group (Shanghai, China) and were reagent grade. Styrene and MMA were .purified by washing with an aqueous solution of sodium hydroxide (5 wt %) three times and deionized water repeatedly until the pH value of the washing water was reduced to 7, dried over anhydrous magnesium sulfate overnight, and then distilled over calcium hydride under vacuum. MAn, BPO, and AIBN were purified by recrystallization from chloroform or ethanol. Toluene and 1,4-dioxane were dried over calcium hydride for 1 week and then distilled over calcium hydride under vacuum. Hydroxyethyl methacrylate (HEMA, 97%) was purchased from Aldrich and used as received. (Heptadecafluoro-1,1,2,2-tetrahydrodecyl) triethoxysilane (>95%) was purchased from Alfa Aesar. A liquid diglycidyl ether of bisphenol A-type epoxy resin (E-44), was purchased from Heli Resin Co., Ltd. (Suzhou, China). Triethanolamine (TEA, >98%), the hardener, was purchased from China Medicine Group (Shanghai, China). Two types of poly(styrene-*co*-maleic anhydride) (SMA) were used for the synthesis of the polymerizable polysoap in this study. One was a commercial product (M_n = 1600, styrene:maleic anhydride = 1.3:1, cumene terminated, Aldrich, denoted as SMA1 in this article), the other one (SMA2, $M_n = 3.4 \times 10^4$, M_w/M_n = 1.74) was synthesized by the copolymerization of styrene and MAn in toluene with AIBN as the initiator (see Supporting Information, Figure S1).

Scheme 1. Synthesis of the Polymerizable Polysoap and Preparation of the Functionalized MWNTs[a]

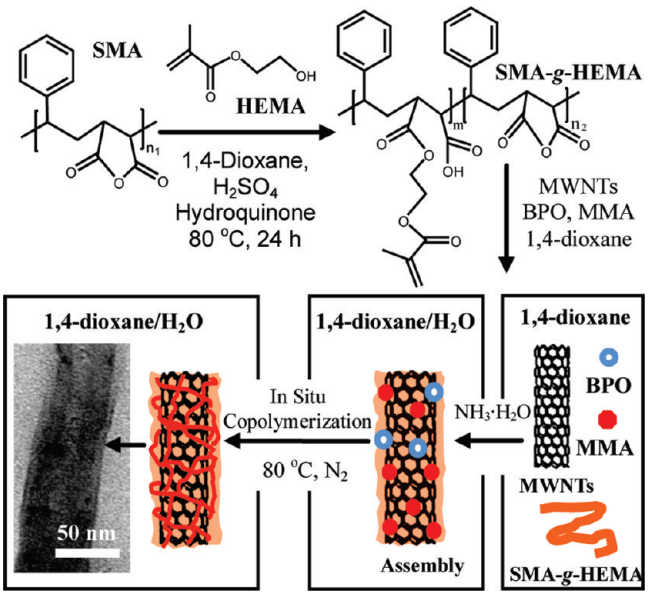

[a] Abbreviations: SMA, poly(styrene-*co*-maleic anhydride); HEMA, hydroxyethyl methacrylate; SMA-*g*-HEMA, SMA grafted with HEMA, i.e. the polymerizable polysoap; BPO, benzoyl peroxide; MMA, methyl methacrylate.

Synthesis of the Polymerizable Polysoap. As schematically shown in Scheme 1, the polymerizable polysoap was synthesized by grafting the side chain of SMA1 and SMA2 with HEMA by esterification reaction in anhydrous 1,4-dioxane (see Supporting Information for detail). A few drops of concentrated H_2SO_4 were added as a catalyst. The polysoaps are denoted as SMA1-*g*-HEMA and SMA2-*g*-HEMA, respectively.

SMA1-g-HEMA. Yield 78%. ^{1}H NMR (500 MHz, d_6-DMSO, ppm): δ = 1.85 (s, 3H, CH_3), 4.10−4.35 (m, 4H, CH_2-O), 5.70 (s, 1H, C*H*=), 6.05 (s, 1H, C*H*=). FTIR (KBr, cm^{-1}): 1169 (acrylic C−O), 1638 (C=C), 1718 (C=O). $M_n = 2.6 \times 10^2$, M_w/M_n = 1.81.

SMA2-g-HEMA. Yield 71%. ^{1}H NMR (500 MHz, d_6-DMSO, ppm): δ = 1.85 (s, 3H, CH_3), 4.10−4.35 (m, 4H, CH_2−O), 5.70 (s, 1H, C*H*=), 6.05 (s, 1H, C*H*=). FTIR (KBr): 1176 (acrylic C−O), 1630 (C=C), 1725 (C=O). $M_n = 4.9 \times 10^4$, M_w/M_n = 2.26.

Synthesis of the Functionalized MWNTs. The recipe for the preparation of the functionalized MWNTs (f-MWNTs) is summarized in Table 1. MWNTs functionalized by SMA1-*g*-HEMA and SMA2-*g*-HEMA and by copolymerizing SMA2-*g*-HEMA with two different amounts of MMA were denoted as f1-MWNTs, f2-MWNTs, f3-MWNTs and f4-MWNTs, respectively. As shown in Scheme 1, MWNTs, SMA-*g*-HEMA, the initiator BPO, and MMA (for f3-MWNTs and f4-MWNTs) were mixed in 1,4-dioxane (50 g) and magnetically stirred at room temperature overnight. When 0.15 g of ammonium hydroxide (26 wt %) was added to the suspension, precipitation appeared immediately. Then, 150 g of deionized water purged with high purity nitrogen for 30 min was added and the suspension was magnetically stirred for 24 h and sonicated for 60 min in a bath sonicator (EQ-50E, 50W, 40 kHz, Shumei, Kunshan, China). Uniform and stable black-colored

Table 1. Recipe for the Preparation of f1-MWNTs, f2-MWNTs, f3-MWNTs, f4-MWNTs, c1-MWNTs, and c2-MWNTs

	amount (g)					
component	f1-MWNTs	f2-MWNTs	f3-MWNTs	f4-MWNTs	c1-MWNTs	c2-MWNTs
MWNTs	0.5	0.5	0.5	0.5	0.5	0.5
SMA1-*g*-HEMA	1.0				1.0	
SMA2-*g*-HEMA		1.0	0.6	0.6		1.0
MMA			0.4	0.8		
BPO	0.02	0.02	0.02	0.02		
1, 4-dioxane	50	50	50	50	50	50
H_2O	150	150	150	150	150	150
$NH_3 \cdot H_2O$	0.15	0.15	0.09	0.09	0.15	0.15

suspensions were thus obtained, in which MWNTs were noncovalently modified by the polymerizable polysoap or the polysoap/MMA mixture due to the hydrophobic effect in water. The suspension was then heated to 80 °C and kept stirring for 24 h under the protection of nitrogen to obtain the functionalized MWNTs.

Preparation of Noncovalently Functionalized MWNTs. Two noncovalently functionalized MWNTs were prepared as control samples for comparison. SMA1-*g*-HEMA and SMA2-*g*-HEMA were simply mixed with MWNTs at a weight ratio of 2:1 in the 1,4-dioxane/water mixture to obtain c1-MWNTs and c2-MWNTs, respectively. BPO was not added, and the suspension was also not heated for polymerization.

Purification of the Samples. The as-prepared suspensions were diluted in distilled water to a solid content of about 0.1 wt % and then vacuum filtered through poly(vinylidene fluoride) microfiltration membranes with an average pore size of 0.45 μm. The filtered solids were collected and redispersed in a 0.2 wt % aqueous solution of NaOH (a good solvent of SMA-*g*-HEMA) by stirring for 10 min and sonication (50 W) for about 60 s. After the filtration and redispersion were repeated 5 times under ambient conditions, the products were washed by deionized water until the pH of the filtrate reached 7 and finally vacuum-dried at 70 °C for 24 h. It should be noted that, for c1-MWNTs and c2-MWNTs, especially for the first three cycles of filtration and redispersion, the filtration rate decreases rapidly with time, therefore, microfiltration membranes were changed about every 1 h.

Preparation of Epoxy/f-MWNTs Nanocomposites. Three types of nanotubes were used to prepare epoxy nanocomposites for a comparison study. One is the oxidized or carboxylated MWNTs prepared by the well-known oxidizing method in a mixture of concentrated nitric acid and sulfuric acid. The second one is c2-MWNTs, the noncovalently functionalized MWNTs. The third one is f3-MWNTs. The content of the nanotubes in all three samples is fixed to be 1 wt %. The MWNTs and epoxy (10 g) were mixed in acetone (10 g) by mechanical stirring and sonication. Acetone was removed by drying at 60 °C overnight and then vacuum drying at 90 °C for 3 days. The curing agent TTA was rapidly added and rigorously stirred. The mixtures were heated to 100 °C and poured into steel molds, degassed, and then heated to 160 °C for 6 h to complete the curing reaction. To observe the dispersion of the nanotubes in the nanocomposites by optical microscopy, a drop of the mixtures was sandwiched between two glass slides and pressed into thin films with a thickness of about 0.1 mm, and heated to 160 °C for 6 h to obtain the thin film of the composites.

Characterization. The chemical structures of pristine MWNTs (p-MWNTs) and the functionalized MWNTs (f1-MWNTs, f2-MWNTs, f3-MWNTs and f4-MWNTs) were characterized by Fourier transform infrared (FTIR) spectroscopy using KBr pellets on a Vector-22 FTIR spectrometer (Bruker, Germany). A spectrum of KBr pellet was recorded as a reference. Hydrogen nuclear magnetic resonance (^{1}H NMR) measurements were carried out on a Varian Mercury Plus 500 MHz spectrometer. The morphologies of the specimens was observed by field emission scanning electron microscopy (FE-SEM, S4800, Hitachi, Japan) at an accelerating voltage of 10 kV and transmission electron microscopy (TEM, JEM 1230, JEOL, JP) operated at 120 kV. Photographs were taken with a digital camera (Kodak, P850). The average diameter and diameter distribution of p-MWNTs, c1-MWNTs, c2-MWNTs, f1-MWNTs, f2-MWNTs, f3-MWNTs, and f4-MWNTs were determined by image analysis of the SEM images using an Image-Pro Plus 5.0 software (Media Cybernetics, USA). Raman spectra were recorded by an ALMEGA-Dispersive Raman (Thermo Nicolet, USA) with 514.5 nm excitation. The solubility of the functionalized MWNTs in deionized water was determined as follows: 0.2 g of f-MWNTs was added to 50 mL of deionized water and sonicated at 50 W for 2 h to obtain a saturated aqueous solution of the f-MWNTs. The suspensions were allowed to stand 3 days at ambient temperature. Five mL of the suspension of the upper layer was taken out with a syringe and vacuum-dried at 80 °C until a constant weight was achieved. Thermogravimetric (TG) analysis was performed on a Pyris 1 thermogravimetric analyzer (Perkin-Elmer, USA) under nitrogen atmosphere. The samples were first heated to 100 °C from room temperature and maintained for 10 min to remove adsorbed water, and then heated to 800 °C at a rate of 20 °C/min. The TG curves for pristine MWNTs, pure polysoaps, the poly(polysoap)s and poly(polysoap-*co*-MMA)s prepared in the absence of MWNTs were recorded as the references when calculating the weight percent of grafted polymer. It should be noted that, different from some polymers that are pyrolyzed almost completely at 800 °C in nitrogen, the polysoaps, poly(polysoap)s, and poly(polysoap-*co*-MMA)s have relatively high residual weights at 800 °C that can not be totally ignored; therefore, the weight percent of the grafted polymer ($W_{\text{grafted polymer}}$) on the surface of the functionalized MWNTs is calculated according to

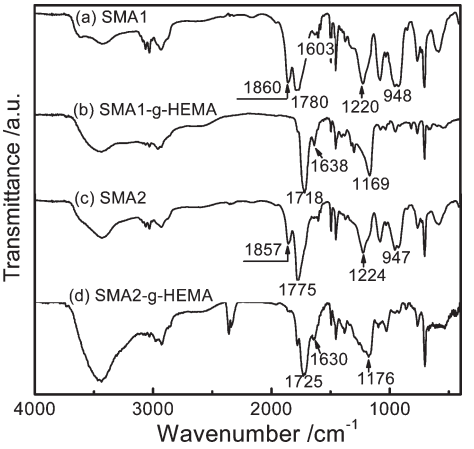

Figure 1. FTIR spectra of the polysoaps and the polymerizable derivatives: (a) SMA1, (b) SMA1-*g*-HEMA, (c) SMA2, and (d) SMA2-*g*-HEMA.

$$W_{\text{grafted polymer}} = \frac{RW_{\text{p-MWNTs}} - RW_{\text{f-MWNTs}}}{RW_{\text{p-MWNTs}} - RW_{\text{pure polymer}}} \times 100 \quad (1)$$

in which, $RW_{\text{p-MWNTs}}$, $RW_{\text{f-MWNTs}}$, and $RW_{\text{pure polymer}}$ are the residual weight percent at 800 °C of pristine MWNTs, the functionalized MWNTs, and their corresponding pure poly(polysoap)s or poly(polysoap-*co*-MMA)s prepared in the absence of MWNTs, respectively.

The grafting efficiency (E) is calculated by

$$E = \frac{W_{\text{grafted polymer}}}{100 - W_{\text{grafted polymer}}} \times \frac{w_{p\text{-}MWNTs}}{w_{polysoap+monomer}} \times 100 \quad (2)$$

in which $w_{\text{p-MWNTs}}$ and $w_{\text{polysoap+monomer}}$ are the weight of pristine MWNTs and the total weight of the added polysoap and monomer.

Results and Discussion

Characterization of the Polymerizable Polysoap. The chemical structure of SMA and the polymerizable polysoap obtained by the esterification reaction between SMA and HEMA was characterized by FTIR, as shown in Figure 1. For SMA1, the adsorption bands at about 1860 and 1780 cm^{-1} can be ascribed to the cyclic anhydride C=O of the maleic anhydride unites, and 1220 cm^{-1} can be ascribed to the cyclic C−O−C group of the maleic anhydride unites. After the esterification reaction, these bands disappear, and the new bands appeared at 1718, 1638, and 1169 cm^{-1} can be ascribed to the ester (C=O), vinyl (C=C), and acrylic C−O groups of the grafted HEMA, respectively. This result confirms the formation of the polymerizable polysoap SMA1-*g*-HEMA. Similar result is obtained for SMA2

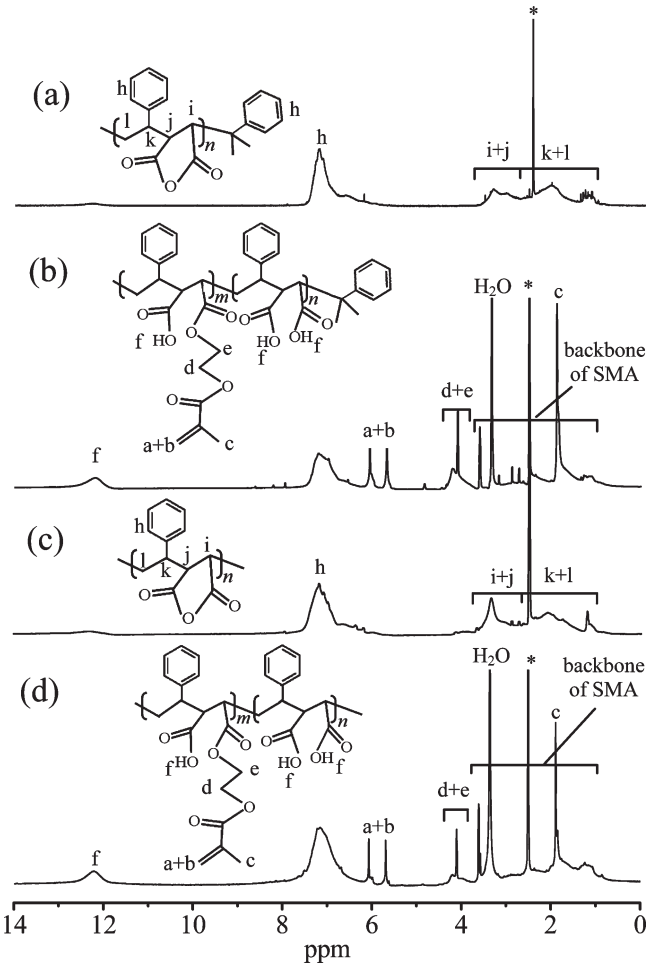

Figure 2. ^{1}H NMR spectra of the polysoaps and the polymerizable derivatives: (a) SMA1, (B) SMA1-*g*-HEMA, (c) SMA2, and (d) SMA2-*g*-HEMA.

and SMA2-*g*-HEMA (Figure 1). Furthermore, in the spectra of the polymerizable polysoaps, the carbonyl stretching band at about 1718 cm^{-1} is due to both esters from HEMA and esters from HEMA adding to MAn. The broad OH stretching band from about 3600 to about 2800 cm^{-1} in all spectra could be due to small amounts of water and to carboxylic acid groups before and after incorporation of HEMA.

The ^{1}H NMR spectra in Figure 2 clearly show the bands of vinyl protons (CH_2=) at 5.70 and 6.05 ppm, the methyl groups ($-CH_3$) at 1.85 ppm, and the methylene protons (CH_2-O) at 4.10−4.35 ppm, further confirming the grafting of HEMA onto SMA macromolecular chains. Moreover, according to the ^{1}H NMR spectra, the molar ratio of HEMA attached to the side chain of SMA can be quantitatively calculated from the integration ratio of the peak at 6.5−7.5 ppm (aromatic ring hydrogens of styrene) and those at 5.7 and 6.05 ppm. The molar ratios of HEMA to MAn in the copolymers are about 68 mol % and 53 mol % for SMA1-*g*-HEMA and SMA2-*g*-HEMA, respectively.

To determine whether the polysoap is polymerizable, 2.0 g of SMA1-*g*-HEMA or SMA2-*g*-HEMA and 0.02 g of BPO were resolved in 10 g of 1,4-dioxane and heated to 80 °C under nitrogen protection, and the polymerization was allowed to proceed for 24 h. For both SMA1-*g*-HEMA and SMA2-*g*-HEMA, gels formed (Supporting Information, Figure S2), confirming that the two polysoaps are polymerizable and cross-linkable because there are multiple double bonds in their macromolecules.

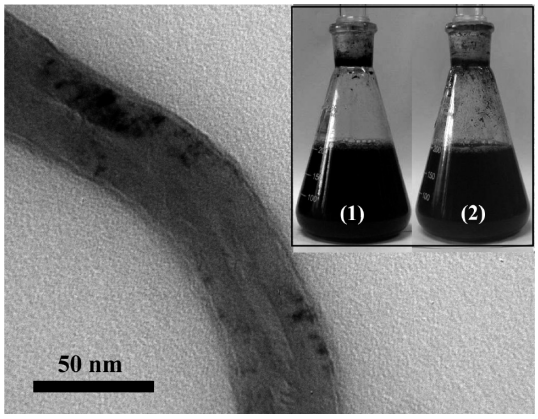

Figure 3. TEM image of a MWNT encapsulated by a thin layer of SMA1-*g*-HEMA. The inset shows photographs of the suspensions of SMA1-*g*-HEMA and MWNTs in the 1, 4-dioxene/water mixture before (1) and after (2) polymerization. The suspension remains stable during the polymerization procedure. All other samples are also stable throughout the polymerization procedure.

The polymerizable polysoaps does not dissolve directly in water, but is soluble in some organic solvents, such as 1, 4-dioxane, acetone and ethanol. By the solvent-exchange method, polysoap-micellized MWNTs can be obtained by the self-assembly of MWNTs and the polysoaps. MWNTs were first dispersed in the 1,4-dioxane solution of the polysoaps and then added to the diluted aqueous solution of ammonia. MWNTs are thus micellized by the polysoaps, because of the hydrophobic effect in the selective solvent and possible $\pi-\pi$ interaction between the nanotube sidewall and the polysoaps. Figure 3 presents a typical TEM image of a nanotube encapsulated by SMA1-*g*-HEMA, in which the ratio between SMA1-*g*-HEMA and MWNTs is 0.8:1. It is shown that the polysoap can form a very uniform thin coating on the surface of MWNTs. This presents an evidence for the formation of polysoap-micellized MWNTs. Because of the strong repulsion between the negatively charged surfaces, the polysoap-micellized MWNTs suspend stably in the 1,4-dioxane/water mixture. It was observed that when the weight ratio between the polysoaps and MWNTs is above 0.6:1, the ink-like suspensions are very uniform and stable. Adding appropriate amount of monomer MMA for the preparation of f3-MWNTs and f4-MWNTs does not bring about instability of the suspension. Moreover, all the suspensions remain stable throughout the followed polymerization procedure, and no precipitation or agglomeration of the MWNTs could be observed, as shown in the inset of Figure 3.

Characterization of the Functionalized MWNTs. Previous studies have shown that both small molecular and macromolecular free radicals can be covalently attached to the sidewall of CNTs.[10−13] Because there are multiple double bonds in the molecules of the polysoaps, it is reasonable to expect that upon polymerization/copolymerization, the poly(polysoap) or poly(polysoap-*co*-MMA) coating on the surface of MWNTs is not only cross-linked but also covalently attached to MWNTs by free radical addition reaction, giving rise to robust polymer-functionalized MWNTs. In addition, Raman spectroscopy was widely used to demonstrate the covalent bonding of chemicals on the surface of carbon nanotubes. The peaks at about 1328 and 1588 cm^{-1} of the Raman spectra belong to the D- and G-bands, respectively. Generally, the G-band is attributed to the crystalline graphitic carbon in CNTs, while the D-band is attributed to the defects in the graphite sheets, sp^3 carbon or some other impurities. The D- to G-band intensity ratio (I_D/I_G) is increased as the result of covalent grafting of free

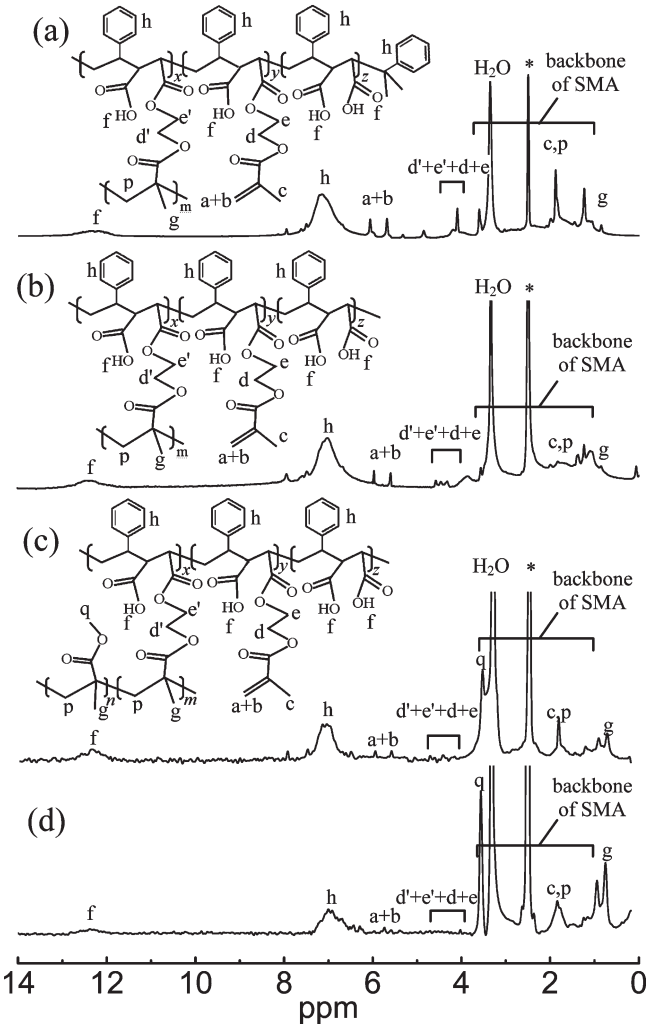

Figure 4. ^{1}H NMR spectra of f1-MWNTs, f2-MWNTs, f3-MWNTs, and f4-MWNTs after rigorous purification. f1-MWNTs and f2-MWNTs are grafted with SMA1-*g*-HEMA and SMA2-*g*-HEMA, respectively. f3-MWNTs and f4-MWNTs are grafted with the copolymer of MMA with SMA1-*g*-HEMA and SMA2-*g*-HEMA, respectively.

radicals onto the sidewall of carbon nanotubes due to the increase of sp^3 bond fraction.[13] Figure S3 presents the Raman spectra of pristine MWNTs and the functionalized MWNTs after purification. It is shown that the intensity ratios of the D- to G-bands increase from 1.18 to 1.34−1.42 after the polymerization of the polysoaps or the copolymerization between the polysoaps and MMA. Because the f-MWNTs were prepared under very mild conditions and no harsh oxidants were used, the obviously increased I_D/I_G values should be associated with the increase of sp^3 bond fraction on the graphite sheets of the functionalized MWNTs resulting from the covalent grafting of the polysoap and poly(polysoap-*co*-MMA) onto MWNTs by free-radical addition reaction.

The existence of the grafted poly(polysoap)s or poly(polysoap-*co*-MMA)s on the surface of MWNTs after rigorous purification is further demonstrated by FTIR and ^{1}H NMR spectra as shown in Figure S4 and Figure 4, respectively. The new band at about 1725 cm^{-1} in Figure S4, which obviously increases for the functionalized MWNTs especially for f3-MWNTs and f4-MWNTs, can be ascribed to the ester C═O groups in the polysoap and MMA (for f3-MWNTs and f4-MWNTs). Note that all the samples have been strictly purified. This again confirms the existence of grafted poly(polysoap)s and poly(polysoap-*co*-MMA)s on the surface of functionalized MWNTs.

The ^{1}H NMR spectra in Figure 4 shows that the bands at 5.70 and 6.05 ppm (vinyl protons) of the functionalized MWNTs become much smaller than those of pure polysoaps (Figure 2). This suggests that the vinyl groups are consumed by the polymerization and copolymerization. For f1-MWNTs and f2-MWNTs, only a part of the vinyl groups is consumed, because of the low reactivity of the polysoaps and the low conversion of their homopolymerization. This result is similar to previous studies show the low reactivity of some other macromonomers.[21] In contrast, for f3-MWNTs and f4-MWNTs, the bands at 5.70 and 6.05 ppm almost disappear, indicating that almost all vinyl groups take part in the copolymerization with MMA. The strong peak appears at 3.6 ppm is due to the methyl protons (−COOCH_3) of the PMMA segments in f3-MWNTs and f4-MWNTs. Before polymerization, the peak at 1.85 ppm is for the methyl groups (−CH_3) attached to the vinyl groups (Figure 2). After polymerization, it becomes smaller while a new peak at 0.74 ppm becomes much stronger, because of the polymerization of the vinyl groups. In addition, the bands at 7.1−7.5 ppm (benzene rings) for f3-MWNTs and f4-MWNTs is also relatively smaller than those of the polysoaps, f1-MWNTs and f2-MWNTs. These phenomena definitely confirm the occurrence of copolymerization between the SMA-*g*-HEMA and MMA in f3-MWNTs and f4-MWNTs. Besides the cross-linked copolymer between the polysoap and MMA, the homopolymer of MMA may also exist in the shells of the functionalized MWNTs. Because the amount of MMA is close to that of polysoap, and the chemical structure of the methacrylate groups of the polysoap is the same with that of MMA, the amount of homopolymer of MMA should be limited. Moreover, some of the homopolymers should be grafted to the nanotube surface, while some of them should be not grafted. Further investigation is necessary to illuminate the details on the composition of the polymeric coatings on the surface of functionalized MWNTs.

Morphology of the Functionalized MWNTs. In this study, MWNTs are first noncovalently functionalized by the assembly of MWNTs and the polymerizable polysoaps in the selective solvent. The micellized MWNTs exhibit good suspendability in the 1,4-dioxane/water mixture. However, as is well-known, the interaction between CNTs and the amphiphilic coatings of such noncovalently functionalized CNTs is relatively weak; therefore, the noncovalently functionalized CNTs may be not satisfactory for applications as fillers of polymeric nanocomposites.

On the other hand, supramolecular chemistry has shown that micelles, vesicles, nanofibers or ultrathin films can be prepared by the self-assembly of surfactants (including both common surfactants and polymerizable ones), block copolymers, and amphiphilic polymers through weak and reversible noncovalent intermolecular forces, such as electrostatic or hydrogen bonding, metal coordination, hydrophobic or van der Waals forces, and $\pi-\pi$ interactions. Numerous studies[22] have demonstrated that covalent cross-linking or polymerization is effective for the permanent stabilization of the structure of the assemblies. Murphy et al.[23] reported the use of a polymerizable surfactant for the decoration of gold nanoparticles or nanorods. After "fixing" the surfactant bilayer by polymerization, the final nanoparticles or nanorods with the polymerized bilayer showed remarkable stability against dialysis, centrifugation-resuspension cycles, and extraction with organic solvent. To overcome the low structure stability of noncovalently modified CNTs, Taton et al.,[24] in their study of poly(styrene)-*block*-poly(acrylic acid) encapsulated SWNTs

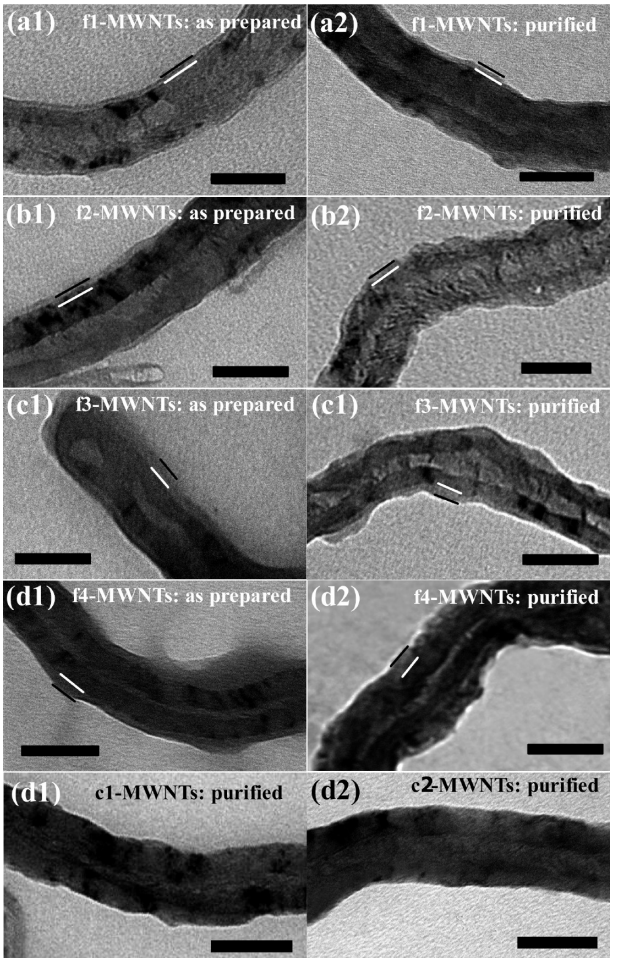

Figure 5. TEM images of (a1, a2) f1-MWNTs, (b1, b2) f2-MWNTs, (c1, c2) f3-MWNTs, (d1, d2) f4-MWNTs, before (left row) and after (right row) rigorous purification; (e and f) purified c1-MWNTs and purified c2-MWNTs, respectively (scale bar = 50 nm).

in a water/dimethylformamide mixture, permanently cross-linked the poly(acrylic acid) shells by adding a water-soluble diamine linker and a carbodiimide activator, which led to the stabilization of the structure of the micelle encapsulated nanotubes. The lyophilized products could be easily redispersed in some organic solvents and polymer solutions with brief sonication. Choi et al.[3] modified SWNTs by in situ free radical polymerization of small molecular weight cationic surfactants that have polymerizable counterions. The SWNTs are encapsulated by the polymerized surfactant layer. The freeze-dried SWNTs are highly dispersible and exist mostly as individually isolated nanotubes in water or alcohols. These studies demonstrate that the structure of noncovalently functionalized CNTs or other nanomaterials can be stabilized by the cross-linking or polymerization of the polymer layer.

According to this scenario, it is expectable that polymerization of the polysoap or copolymerization of the polysoap with MMA on the nanotube surface will also increase the structural stability of the functionalized MWNTs in this study. The aforementioned Raman, FTIR, and ^{1}H NMR results have demonstrated that the poly(polysoap)s and poly(polysoap-*co*-MMA)s have been grafted onto the surface of MWNTs. To further understand the influence of polymerization/copolymerization on the structural stability of the functionalized MWNTs, we observe the morphologies of the functionalized MWNTs by TEM before and after rigorous purification and compared with those of the controll samples, as shown in Figure 5. Before purification, the functionalized MWNTs are encapsulated by a very uniform layer of light-colored polymer sheath. The thickness of the polymer sheath of f4-MWNTs is obviously larger than those of other samples. This is because the amount of polysoap and MMA of f4-MWNTs is larger than of other samples. The polymer sheath becomes deformed and less uniform after the rigorous purification and drying, most likely because the polymer sheath contains large amount of hydrophilic groups, thus can be swelled by water. But fortunatly, the polymer sheaths are not detached seriously from MWNTs. On the contrary, as shown in Figure 5e and 5f, the control samples c1-MWNTs and c2-MWNTs become clean after purification, suggesting that the polymer sheaths are mostly removed by washing because of the instability of the noncovalently adsorbed polymer sheaths. This result demonstrates that the structural stability of the polysoap-functionalized MWNTs is greatly increased by the polymerization of the polysoaps or the copolymerization between SMA-*g*-HEMA and MMA *in situ* on the surface of MWNTs.

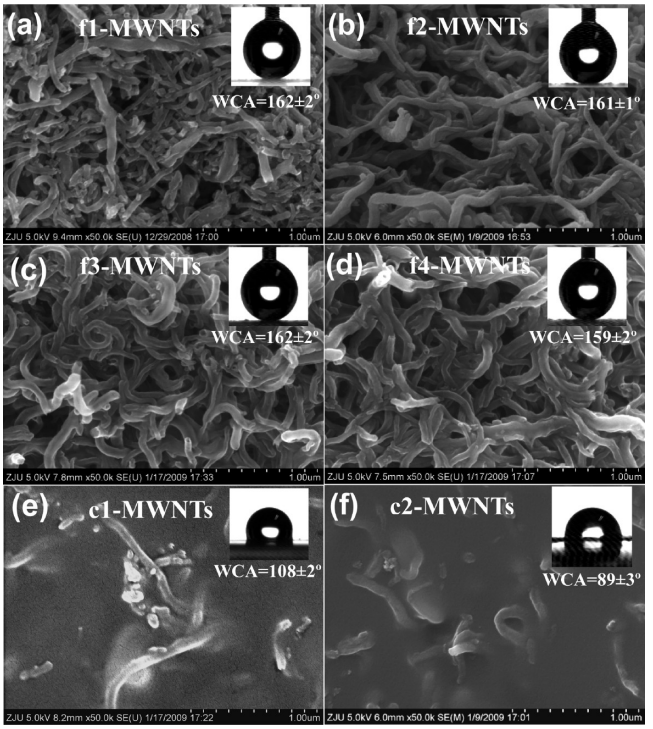

Figure 6. Morphology of (a) f1-MWNTs, (b) f2-MWNTs, (c) f3-MWNTs, (d) f4-MWNTs, (e) c1-MWNTs, and (f) c2-MWNTs, solution-cast from their as-prepared suspensions and dried at 80 °C. The insets present the profile of water droplets on the surfaces after fluoroalkylsilane treatment. The volume of water droplets is fixed to 4 μL.

SEM was used to further observe the morphologies of the functionalized MWNTs and control samples after their as-prepared suspensions were solution-cast on aluminum foils and dried at 80 °C directly. The functionalized MWNTs (Figure 6a−d) in the cast films are fibrous with a diameter somewhat larger than that of pristine MWNTs (see the Suporting Information). This surports the sepculation that the polymer sheath on the nanotubes are cross-linked. Moreover, it should be noted that almost no free polymer globules can be observed in the SEM images. This suggests that the polymerization of the polysoaps or the copolymerization of the polysoaps and MMA occurs primarily on the surface of MWNTs, or in other words, the amount of free polymers (i.e., polymers not attached covalently to the nanotube surfaces)

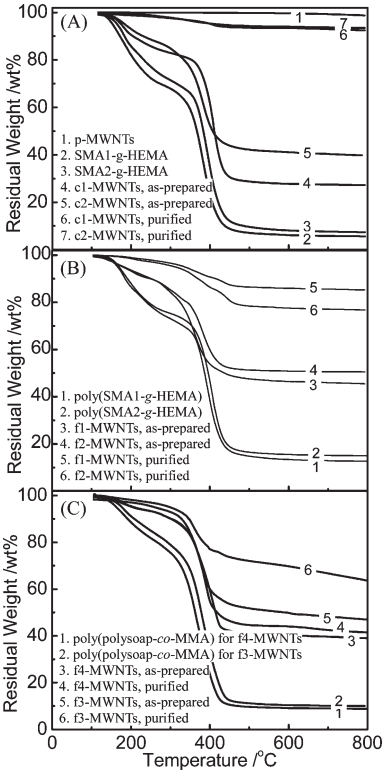

Figure 7. TG curves for (A) pristine MWNTs, the polysoaps, and c1-MWNTs and c2-MWNTs before and after purification, (B) the pure poly(SMA1-*g*-HEMA), poly(SMA2-*g*-HEMA), and f1-MWNTs and f2-MWNTs before and after purification, and (C) the pure poly(polysoap-*co*-MMA)s (i.e., the copolymers of MMA and SMA2-*g*-HEMA) for f3-MWNTs and f4-MWNTs, as well as f3-MWNTs and f4-MWNTs before and after purification.

in the reaction system should be rather limited. As to the control samples, in contrast, the polysoaps detach from the nanotube surface, and fuse into continuous phase, in which the nanotubes are embedded (Figure 6e,f), because the polymer is not cross-linked and not grafted onto the surface of MWNTs.

In considering that the fibrious polysoap-encapsulated MWNTs form a highly porous network morphology, which can be used as a platform for constructing superhydrophobic coatings, we coated the surfaces of cast films with a fluoroalkylsilane. As expected, the cast films exhibit superhydrophobicity with water contact angles (WCAs) above $159 \pm 2°$ (Figure 6 insets). On the contrary, the cast films of the control samples are not superhydrophobic after the fluoroalkylsilane treatment, because the film surfaces are not highly porous (Figure 6e,f). This result further confirms the significantly increased structural stability of the cross-linked sheath of the polysoap functionalized MWNTs upon drying, and suggests that the functionalized MWNTs can be used as new building blocks for constructing superhydrophobic surfaces by simple brush coating or spraying, followed by coating with low surface energy materials.

TG Analysis. To further quantitatively determine the structural stability of the polymer sheath on the surface of MWNTs, TG analysis is used to measure the amount of polymers attached to the surface of the MWNTs before and after rigorous purification, as shown in Figure 7. In good agreement with the result of TEM observation, the polymers on the control samples c1-MWNTs and c2-MWNTs are mostly removed after the rigorous purification. The weight percent of the residual polymers after rigorous purification is only 5.3 and 6.9 wt % for the c1-MWNTs and c2-MWNTs, respectively. In contrast, the weight percent of the residual grafted polymers for f1-MWNTs, f2-MWNTs, f3-MWNTs, and f4-MWNTs are increased to 15.7, 26.3, 39.1, and 64.7 wt %, respectively, which are significantly higher than of the control samples. The percent retention (R), which is defined as the ratio of the amount of poly(polysoap) or poly(polysoap-*co*-MMA) retained on MWNTs after purification to that before purification (times 100), is calculated to characterize the structural stability of the functionalized MWNTs. As shown in Table 2, R is only 8.4% and 8.9% for c1-MWNTs and c2-MWNTs, respectively, indicating that most polysoaps were removed from the nanotube surface after the purification process because of the relatively weak noncovalent interaction between the polysoap and the nanotubes. In contrast, R is increased to 25.3% and 45.7% for f1-MWNTs and f2-MWNTs, respectively, which is much higher than those of c1-MWNTs and c2-MWNTs. In addition, the weight percent of the grafted polymer and the grafting efficiency of f1-MWNTs are obviously lower than of f2-MWNTs. This is most likely because of the much lower molecular weight of SMA1-*g*-HEMA, which is less favorable for the formation of robust, cross-linked sheath of the micellized MWNTs. This is also the reason SMA2-*g*-HEMA was selected to copolymerize with MMA for the preparation of f3-MWNTs and f4-MWNTs. Moreover, copolymerization of the polysoap with MMA further increases R to 67.6% and 96.1% for f3-MWNTs and f4-MWNTs, respectively, which is much higher than those of f1-MWNTs and f2-MWNTs. These results confirm that the structural stability of the polymer sheath is greatly improved by the polymerization of the polysoaps and the copolymerization between the polysoaps and MMA. Obviously, MMA is more reactive than the polysoaps in the polymerization reaction and facilitates the polymerization/cross-linking of the polymer sheath.

Table 2. Weight Percent (W_p) of Polymer on the MWNTs before and after Purification, the Percent Retention (R) and Grafting Efficiency (E) Calculated from the Result of TG Analysis, and the Solubility in Water

sample code	W_p[a] (wt %)	W_p[b] (wt %)	R (%)	E (%)	solubility (mg/mL)
c1-MWNTs	63	5	8.4		< 0.05
c2-MWNTs	78	7	9.0		< 0.05
f1-MWNTs	62	16	25.8	9.5	0.36
f2-MWNTs	58	26	44.8	17.4	0.29
f3-MWNTs	58	40	69.0	32.9	1.44
f4-MWNTs	68	65	95.6	65.7	4.43

[a] Before purification. [b] After purification.

The differential TG (dTG) curves shown in Figure S5 in the Surpporting Information further presents evidence for the covalent grafting of the poly(polysoap)s or poly(polysoap-*co*-MMA)s on the surface of the MWNTs. For the control samples, the peak pyrolysis temperature of the residual polysoaps on the nanotube surface is only slightly higher or even lower (Figure S5A) than that of pure polysoaps; on the contrary, for the functionalized MWNTs (Figure S5B, C), the highest peak pyrolysis temperature is higher by 11 °C or even 42 °C than their corresponding polymer sheaths in the absence of MWNTs. Similar phenomenon is commonly observed in previously reported polymer-grafted CNTs, and is attributed to the covalent bonding of the polymer coatings to the graphene sidewall of CNTs.[25]

Grafting Efficiency of the Functionalized MWNTs. For common "grafting to" modification of CNTs by free radical polymerization, the polymerization occurs both on nanotube surfaces and in the bulk solution, leading to low grafting efficiency. In this method, MWNTs are first micellized by the polymerizable polysoap, and because of the hydrophobic

interaction, the monomer should be absorbed preferentially by the hydrophobic region of the polysoap coating on the nanotubes surface. As aforementioned, in the SEM images of the as-prepared functionalized MWNTs, almost no free polymer globules can be observed. This suggests that the polymerization/copolymerization occurs primarily on the nanotube surface, although the polymerization/copolymerization in the bulk solution cannot be totally excluded. Moreover, the grafted polymer is cross-linked, such that once a part of the polymer chains are bonded covalently to the sidewall of the nanotubes, the whole polymer sheath is bonded to the nanotubes. Therefore, we believe high grafting efficiency can be obtained by this method.

The grafting efficiency, calculated as the ratio between the quantity of grafted polymer and the total added polysoap or polysoap/MMA, is obtained basing on the result of TG analysis. The amount of grafted polymer on the nanotube surface before and after purification, the percent retention and the grafting efficiency calculated from the result of TG anaylsis are summarized in Table 2. It should be noted that the grafting efficiency of f1-MWNTs and f2-MWNTs is 9.3% and 17.8%, respectively, which is much higher than that obtained by the previously reported "grafting to" methods showing grafting efficiencies below 1% for MWNTs by free radical addition reaction *in situ* in vinyl monomers or in good solvents of the grafted polymers.[14] Moreover, the grafting efficiency for f3-MWNTs and f4-MWNTs is further increased to 32.1% and 65.7%, respectively, the latter of which is much higher than that for SWNTs grafted by polymers in poor solvents,[17] and even much higher than that for polymer-grafted MWNTs obtained by the "grafting from" ATRP or RAFT polymerization.[19] Copolymerization of polysoap and MMA monomer significantly increases the grafting efficiency, which should be also mainly associated with the high reactivity of the monomer. To the best of our knowledge, this study presents the highest grafting efficiency for MWNTs by free radical polymerization/copolymerization.

Redispersibility of the Functionalized MWNTs. The redispersibility of the functionalized MWNTs is investigated. It is found that the drying condition has strong effect on the redispersibility. If the functionalized MWNTs are air-dried under ambient conditions, they can be readily redispersed in many polar solvents, such as water, 1,4-dioxane, ethanol, acetone, dimethylformamide (DMF) after brief sonication, forming uniform and stable suspensions. However, after vacuum drying at 80 °C overnight, the functionalized MWNTs are not redispersible in 1,4-dioxane, ethanol and acetone, but can still be readily redispersed in some strongly polar solvents, such as DMF and water (Surpporting Information, Figure S6) with a relatively high solubility. This phenomenon should be related to the hydrogen bonds among the carboxyl groups formed under relatively high drying temperatures.

The 'solubility' of the functionalized MWNTs (purified and vacuum-dried at 70 °C for 24 h) redispersed in deionized water is 0.36, 0.29, 1.44, and 4.43 mg/mL for f1-MWNTs, f2-MWNTs, f3-MWNTs, and f4-MWNTs, respectively. The "solubility" is much higher than that of the oxidized or carboxylated carbon nanotubes (0.03−0.15 mg/mL) prepared by the well-known oxidizing method in a mixture of concentrated nitric acid and sulfuric acid.[26] Moreover, f3-MWNTs and f4-MWNTs have the higher "solubility" than f1-MWNTs and f2-MWNTs, obviously, copolymerization of the polysoaps with MMA significantly increases the amount of grafted polymers and so the "solubility" of the f-MWNTs. This result is again in good agreement with the result of TG analysis and TEM.

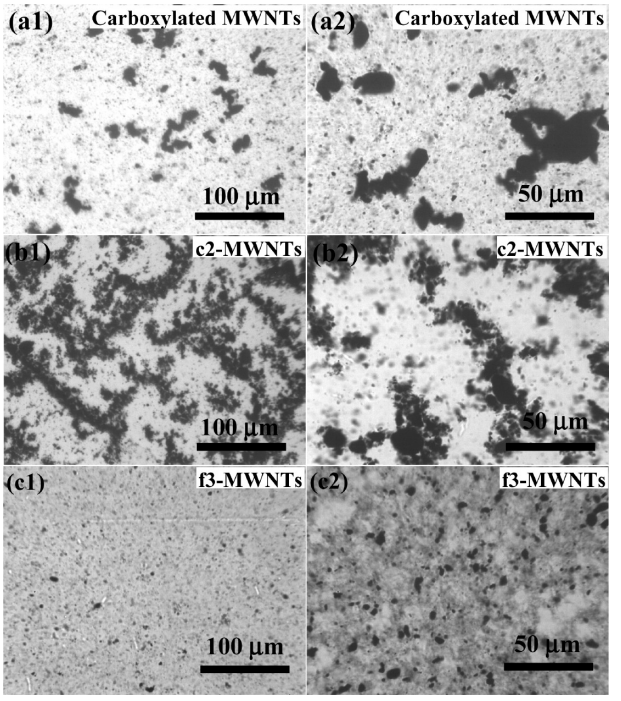

Figure 8. Optical images of the cured epoxy nanocomposites filled with (a1, a2) carboxylated MWNTs, which were prepared by the well-known oxidizing method in a mixture of concentrated nitric acid and sulfuric acid; (b1, b2) MWNTs noncovalently decorated by SMA2-*g*-HEMA by simply mix them in acetone and then added to epoxy oligomer; and (c1, c2) f3-MWNTs at low (left, ×500) and high (right, ×1000), respectively. The concentration of MWCNTs for all the samples are 1 wt %.

Epoxy/f-MWNTs Nanocomposites. To investigate the effect of polymer-grafted MWNTs on the properties of polymer composites, epoxy resin filled with f3-MWNTs was prepared and compared with those filled with carboxylated MWNTs (which is prepared by the well-known acid treatment method), and c2-MWNTs (i.e., MWNTs noncovalently decorated by SMA2-*g*-HEMA), respectively. The dispersion of MWNTs in the epoxy nanocomposites was observed by optical microscopy (Figure 8). It is obvious that after the curing reaction of epoxy, the carboxylated MWNTs and the noncovalently decorated MWNTs aggregate into large clusters of several tens of micrometers. In contrast, although f3-MWNTs also form clusters in the matrices, the size of the clusters is much smaller, indicating the greatly improved dispersion uniformity of the f3-MWNTs. This phenomenon should be related to the stabilized polysoap coatings with large amount of carboxyl groups on the surface of f3-MWNTs.

Figure 9 presents the elastic modulus (E') and tan δ curves of pure epoxy and the nanocomposites filled with carboxylated MWNTs, c2-MWNTs, and f3-MWNTs, respectively. It is found that all the three type of modified MWNTs can increase the storage modulus and the peak temperatures of the tan δ curves of their composites. However, it is noted that f3-MWNTs increase the E' and the peak temperature of the tan δ curve more effectively than the other two samples. The E' value is increased by 11.8%, and the peak temperature of the tan δ curve is increased by 22.8 °C when the amount of nanotubes is only 1 wt %. Nevertheless, the other two samples only show very limited improvement in both dynamic mechanical properties and heat resistance. It is well-known that the carboxyl groups of the carboxylated MWNTs can react with epoxy groups,[27] therefore, all the three types of modified MWNTs should be able to react with epoxy. The reaction between the robust polymer sheath of f3-MWNTs

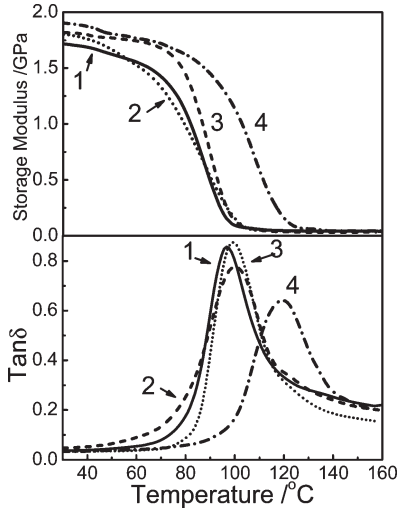

Figure 9. Storage modulus and tan δ curves of pure epoxy resin (1), the nanocomposites filled with carboxylated MWNTs (2), MWNTs noncovalently decorated by SMA2-*g*-HEMA (3), and f3-MWNTs (4), respectively. The content of MWNTs in the nanocomposites is 1 wt %.

and epoxy, together with the greatly improved dispersion uniformity, are definitely responsible for the greatly enhanced dynamic mechanical properties and heat resistance of the nanocomposites.

Conclusions

By simply introducing vinyl groups to SMA by the esterification reaction, a novel polymerizable polysoap was obtained. By a single-step of free radical polymerization/copolymerization in situ on the surface of MWNTs, the poly(polysoap)s and poly(polysoap-*co*-MMA)s are cross-linked and covalently attached to MWNTs. Copolymerization of the polysoap with MMA greatly enhances the structural stability of the functionalized MWNTs, and the grafting efficiency can be as high as 65.7%. This method combines the advantages of noncovalent functionalization (simplicity, mild reaction conditions and ease of scale-up), and the high structural stability of covalent functionalization. Moreover, the functionalized MWNTs increase the dynamic mechanical properties of epoxy more effectively than carboxylated MWNTs and noncovalently functionalized MWNTs. Further investigations will be conducted to find optimal reaction conditions and recipes. Besides MMA, this method can also be applied to many other vinyl monomers. It is also believable that the carboxyl groups of SMA-*g*-HEMA impart the functionalized MWNTs a high reactivity similar to that of acid-functionalized CNTs,[28] which offer a wide variety of possible reactions for further functionalization. The versatility of this method opens up new possibilities of large-scale production of polymer-functionalized MWNTs at low cost.

Acknowledgment. The authors acknowledge the funding support from the National Natural Science Foundation of China (Grants 20574060 and 50773066).

Supporting Information Available: Text discussing the synthesis of SMA and the polymerizable polysoap, figures showing GPC, TEM, SEM and optical images, Raman and FTIR spectra, and calculation of the weight percent of grafted polymer (PDF), and a table of GPC data. This material is available free of charge via the Internet at http://pubs.acs.org.

References and Notes

(1) (a) Sekitani, T.; Someya, T. *Adv. Mater.* **2010**, *22*, 2228–2246. (b) Simmons, T. J.; Bult, J.; Hashim, D. P.; Linhardt, R. J.; Ajayan, P. M. *ACS Nano* **2009**, *3*, 865–870. (c) Pötschke, P.; Zschoerper, N. P.; Moller, B. P.; Vohrer, U. *Macromol. Rapid Commun.* **2009**, *30*, 1828–1833. (d) Kuila, B. K.; Park, K. S.; Dai, L. M. *Macromolecules* **2010**, *43*, 6699–6705.

(2) (a) Sainsbury, T.; Erickson, K.; Okawa, D.; Zonte, C. S.; Fréchet, J. M. J.; Zettl, A. *Chem. Mater.* **2010**, *22*, 2164–2171. (b) Binder, W. H.; Sachsenhofer, R. *Macromol. Rapid Commun.* **2007**, *28*, 15–54. (c) Lee, J. I.; Yang, S. B.; Jung, H. T. *Macromolecules* **2009**, *42*, 8328–8334. (d) Hasan, T.; Tan, P. H.; Bonaccorso, F.; Rozhin, A. G.; Scardaci, V.; Milne, W. I.; Ferrari, A. C. *J. Phys. Chem. C* **2008**, *112*, 20227–20232. (e) Yao, Y.; Li, W. W.; Wang, S. B.; Yan, D. Y.; Chen, X. S. *Macromol. Rapid Commun.* **2006**, *27*, 2019–2025. (f) Backes, C.; Mundloch, U.; Ebel, A.; Hauke, F.; Hirsch, A. *Chem.—Eur. J.* **2010**, *16*, 3314–3317. (l) Grady, B. P. *Macromol. Rapid Commun.* **2010**, *31*, 247–257. (m) Xie, L.; Xu, F.; Qiu, F.; Lu, H. B.; Yang, Y. L. *Macromolecules* **2007**, *40*, 3296–3305. (g) Banerjee, S.; Hemraj-Benny, T.; Wong, S. S. *Adv. Mater.* **2005**, *17*, 17–29. (h) Liu, P. *Eur. Polym. J.* **2005**, *41*, 2693–2703.

(3) (a) Kim, T. H.; Doe, C.; Kline, S. R.; Choi, S. M. *Adv. Mater.* **2007**, *19*, 929–933. (b) Kim, T. H.; Doe, C.; Kline, S. R.; Choi, S. M. *Macromolecules* **2008**, *41*, 3261–3266.

(4) (a) Shin, J. Y.; Premkumar, T.; Geckeler, K. E. *Chem.—Eur. J.* **2008**, *14*, 6044–6048. (b) Angelikopoulos, P.; Bock, H. *J. Phys. Chem. B* **2008**, *112*, 13793–13801.

(5) (a) Richard, C.; Balavoine, F.; Schultz, P.; Ebbesen, T. W.; Mioskowski, C. *Science* **2003**, *300*, 775–778. (b) Qiao, R.; Ke, P. C. *J. Am. Chem. Soc.* **2006**, *128*, 13656–13657.

(6) (a) Etika, K. C.; Jochum, F. D.; Theato, P.; Grunlan, J. C. *J. Am. Chem. Soc.* **2009**, *131*, 13598–13599. (b) Chen, R. J.; Zhang, Y. G.; Wang, D. W.; Dai, H. J. *J. Am. Chem. Soc.* **2001**, *123*, 3838–3839. (c) Meuer, S.; Braun, L.; Zentel, R. *Chem. Commun.* **2008**, 3166–3168.

(7) (a) Mountrichas, G.; Tagmatarchis, N.; Pispas, S. *J. Phys. Chem. B* **2007**, *111*, 8369–8372. (b) Bockstaller, M. R.; Mickiewicz, R. A.; Thomas, E. L. *Adv. Mater.* **2005**, *17*, 1331–1349. (c) Shvartzman-Cohen, R.; Florent, M.; Goldfarb, D.; Szleifer, I.; Yerushalmi-Rozen, R. *Langmuir* **2008**, *24*, 4625–4632.

(8) (a) Artyukhin, A. B.; Bakajin, O.; Stroeve, P.; Noy, A. *Langmuir* **2004**, *20*, 1442–1448. (b) Yang, D. Q.; Rochette, J. F.; Sacher, E. *J. Phys. Chem. B* **2005**, *109*, 4481–4484. (c) Wang, D.; Chen, L. W. *Nano Lett.* **2007**, *7*, 1480–1484. (d) Grunlan, J. C.; Liu, L.; Kim, Y. S. *Nano Lett.* **2006**, *6*, 911–915.

(9) Wang, D.; Ji, W. X.; Li, Z. C.; Chen, L. W. *J. Am. Chem. Soc.* **2006**, *128*, 6556–6557.

(10) (a) Dror, Y.; Pyckhout-Hintzen, W.; Cohen, Y. *Macromolecules* **2005**, *38*, 7828–7836. (b) Han, X. G.; Li, Y. L.; Deng, Z. X. *Adv. Mater.* **2007**, *19*, 1518–1522. (c) Zhao, W.; Gao, Y.; Brook, M. A.; Li, Y. F. *Chem. Commun.* **2006**, 3582–3584.

(11) Lee, N. K.; Abrams, C. F. *J. Chem. Phys.* **2004**, *121*, 7484–7493.

(12) (a) Han, J. K.; Kim, H. J.; Kim, D. Y.; Jo, S. M.; Jang, S. Y. *ACS Nano* **2010**, *4*, 3503–3509. (b) Pompeo, F.; Resasco, D. E. *Nano Lett.* **2002**, *2*, 369–373. (c) Xu, H. X.; Wang, X. B.; Zhang, Y. F.; Liu, S. Y. *Chem. Mater.* **2006**, *18*, 2929–2934. (d) Ying, Y. M.; Saini, R. K.; Liang, F.; Sadana, A. K.; Billups, W. E. *Org. Lett.* **2003**, *5*, 1471–1473. (e) Liao, S. H.; Yen, C. Y.; Hung, C. H.; Weng, C. C.; Tsai, M. C.; Lin, Y. F.; Ma, C. C. M.; Pan, C.; Su, A. *J. Mater. Chem.* **2008**, *33*, 3993–4002. (f) Umek, P.; Seo, J. W.; Hernadi, K.; Mrzel, A.; Pechy, P.; Mihailovic, D. D.; Forró, L. *Chem. Mater.* **2003**, *15*, 4751–4755. (g) Park, S. J.; Cho, M. S.; Lim, S. T.; Choi, H. J.; Jhon, M. S. *Macromol. Rapid Commun.* **2003**, *24*, 1070–1073. (h) Koval'chuk, A. A.; Shevchenko, V. G.; Shchegolikhin, A. N.; Nedorezova, P. M.; Klyamkina, A. N.; Aladyshev, A. M. *Macromolecules* **2008**, *41*, 7536–7542. (i) Sung, J. H.; Kim, H. S.; Jin, H. J.; Choi, H. J.; Chin, I. J. *Macromolecules* **2004**, *37*, 9899–9902.

(13) (a) McIntosh, D.; Khabashesku, V. N.; Barrera, E. V. *J. Phys. Chem. C* **2007**, *111*, 1592–1600. (b) Kitano, H.; Tachimoto, K.; Gemmei-Ide, M.; Tsubaki, N. *Macromol. Chem. Phys.* **2006**, *207*, 812–819.

(14) (a) Chen, S. M.; Wu, G. Z.; Liu, Y. D.; Long, D. W. *Macromolecules* **2006**, *39*, 330–334. (b) Shen, J. F.; Hu, Y. Z.; Qin, C.; Ye, M. X. *Langmuir* **2008**, *24*, 3993–3997.

(15) (a) Liu, Y. Q.; Yao, Z. L.; Adronov, A. *Macromolecules* **2005**, *38*, 1172–1179. (b) Qin, S. H.; Qin, D. Q.; Ford, W. T.; Herrera, J. E.; Resasco, D. E.; Bachilo, S. M.; Weisman, R. B. *Macromolecules* **2004**, *37*, 3965–3967. (c) Qin, S. H.; Qin, D. Q.; Ford, W. T.; Herrera, J. E.; Resasco, D. E. *Macromolecules* **2004**, *37*, 9963–9967.

(16) (a) Tada, K.; Furuya, S.; Watanabe, K. *Phys. Rev. B* **2001**, *63*, 155405. (b) Gulseren, O.; Yildirim, T.; Ciraci, S. *Phys. Rev. Lett.* **2001**, *87*, 116802.

(17) Guo, G. Q.; Yang, D.; Wang, C. C.; Yang, S. *Macromolecules* **2006**, *39*, 9035–9040.
(18) Sakellariou, G.; Ji, H.; Mays, J. W.; Baskaran, D. *Chem. Mater.* **2008**, *20*, 6217–6230.
(19) (a) Kong, H.; Gao, C.; Yan, D. Y. *Macromolecules* **2004**, *37*, 4022–4030. (b) Kong, H.; Gao, C.; Yan, D. Y. *J. Mater. Chem.* **2004**, *14*, 1401–1405. (c) Hong, C. Y.; You, Y. Z.; Pan, C. Y. *Chem. Mater.* **2005**, *17*, 2247–2254.
(20) (a) Pei, X. W.; Hao, J. C.; Liu, W. M. *J. Phys. Chem. C* **2007**, *111*, 2947–2952. (b) Qin, S. H.; Qin, D. Q.; Ford, W. T.; Resasco, D. E.; Herrera, J. E. *J. Am. Chem. Soc.* **2004**, *126*, 170–176. (c) Koval'chuk, A. A.; Shchegolikhin, A. N.; Shevchenko, V. G.; Nedorezova, P. M.; Klyamkina, A. N.; Aladyshev, A. M. *Macromolecules* **2008**, *41*, 3149–3156. (d) Liu, Y. L.; Chen, W. H. *Macromolecules* **2007**, *40*, 8881–8886. (e) Priftis, D.; Petzetakis, N.; Sakellariou, G.; Pitsikalis, M.; Baskaran, D.; Mays, J. W.; Hadjichristidis, N. *Macromolecules* **2009**, *42*, 3340–3346.
(21) (a) Qin, S. H.; Qiu, K. Y. *Chin. J. Polym. Sci.* **2000**, *18*, 515–520. (b) Wood, C. D.; Cooper, A. I. *Macromolecules* **2003**, *36*, 7534–7542. (c) Capek, I.; Riza, M.; Akashi, M. *Makromol. Chem.* **1992**, *193*, 2843–2860.
(22) (a) Chatjaroenporn, K.; Baker, R. W.; FitzGerald, P. A.; Warr, G. G. *Langmuir* **2010**, *26*, 11715–11719. (b) Park, M. K.; Deng, S. X.; Advincula, R. C. *J. Am. Chem. Soc.* **2004**, *126*, 13723–13731. (c) Kang, Y. J.; Taton, T. A. *Angew. Chem., Int. Ed.* **2005**, *44*, 409–412. (d) Liu, G. J.; Yan, X. H. *Polymer* **2003**, *44*, 7721–7727. (e) Yan, X. H.; Liu, F. T.; Li, Z.; Liu, G. J. *Macromolecules* **2001**, *34*, 9112–9116. (f) Stewart, S.; Liu, G. J. *Angew. Chem., Int. Ed.* **2000**, *39*, 340–344. (g) Luo, S. Z.; Xu, J.; Zhang, Y. F.; Liu, S. Y.; Wu, C. *J. Phys. Chem. B* **2005**, *109*, 22159–22166. (h) Jiang, X. Z.; Zhang, G. Y.; Narain, R.; Liu, S. Y. *Langmuir* **2009**, *25*, 2046–2054. (i) Joralemon, M. J.; O'Reilly, R. K.; Hawker, C. J.; Wooley, K. L. *J. Am. Chem. Soc.* **2005**, *127*, 16892–16899.
(23) (a) Alkilany, A. M.; Murphy, C. J. *Langmuir* **2009**, *25*, 13874–13879. (b) Alkilany, A. M.; Nagaria, P. K.; Wyatt, M. D.; Murphy, C. J. *Langmuir* **2010**, *26*, 9328–9333.
(24) Kang, Y. J.; Taton, T. A. *J. Am. Chem. Soc.* **2003**, *125*, 5650–5651.
(25) (a) Gao, J. B.; Itkis, M. E.; Yu, A. P.; Bekyarova, E.; Zhao, B.; Haddon, R. C. *J. Am. Chem. Soc.* **2005**, *127*, 3847–3854. (b) Sun, G. X.; Chen, G. M.; Liu, Z. P.; Chen, M. *Carbon* **2010**, *48*, 1434–1440. (c) Sarno, M.; Gorrasi, G.; Sannino, D.; Sorrentino, A.; Ciambelli, P.; Vittoria, V. *Macromol. Rapid Commun.* **2004**, *25*, 1963–1967.
(26) Zhao, W.; Song, C.; Pehrsson, P. E. *J. Am. Chem. Soc.* **2002**, *124*, 12418–12419.
(27) (a) Tsyalkovsky, V.; Klep, V.; Ramaratnam, K.; Lupitskyy, R.; Minko, S.; Luzinov, I. *Chem. Mater.* **2008**, *20*, 317–325. (b) Liu, Y.; Klep, V.; Zdyrko, B.; Luzinov, I. *Langmuir* **2005**, *21*, 11806–11813. (c) Lokitz, B. S.; Messman, J. M.; Hinestrosa, J. P.; Alonzo, J.; Verduzco, R.; Brown, R. H.; Osa, M.; Ankner, J. F.; Kilbey, S. M., II *Macromolecules* **2009**, *42*, 9018–9026. (d) Dispenza, C.; Spadaro, G.; McGrail, P. T. *Macrom. Chem.Phys.* **2005**, *206*, 393–403. (e) Shimokawa, T.; Shinmoto, Y.; Kameyama, A.; Nishikubo, T. J. *Polym. Sci. A: Polym. Chem.* **1996**, *34*, 1951–1957.
(28) (a) Wang, W.; Fernando, K. A. S.; Lin, Y.; Meziani, M. J.; Veca, L.; Cao, L. M.; Zhang, P. Y.; Kimani, M. M.; Sun, Y. P. *J. Am. Chem. Soc.* **2008**, *130*, 1415–1419. (b) Fu, K. F.; Li, H. P.; Zhou, B.; Kitaygorodskiy, A.; Allard, L. F.; Sun, Y. P. *J. Am. Chem. Soc.* **2004**, *126*, 4669–4675. (c) Lin, Y.; Meziani, M. J.; Sun, Y. P. *J. Mater. Chem.* **2007**, *17*, 1143–1148. (d) Homenick, C. M.; Sheardown, H.; Adronov, A. *J. Mater. Chem.* **2010**, *20*, 2887–2894. (e) Ge, J. J.; Zhang, D.; Li, Q.; Hou, H. Q.; Graham, M. J.; Dai, L. M.; Harris, F. W.; Cheng, S. Z. D. *J. Am. Chem. Soc.* **2005**, *127*, 9984–9985. (f) Zhang, Y. C.; Broekhuis, A. A.; Stuart, M. C. A.; Landaluce, T. F.; Fausti, D.; Rudolf, P.; Picchioni, F. *Macromolecules* **2008**, *41*, 6141–6146.